Enhancement of coenzyme binding by a single point mutation at the coenzyme binding domain of *E. coli* lactaldehyde dehydrogenase

JOSÉ SALUD RODRÍGUEZ-ZAVALA

Departamento de Bioquímica, Instituto Nacional de Cardiología "Ignacio Chávez," Tlalpan D.F. 14080, Mexico

(RECEIVED October 3, 2007; FINAL REVISION November 20, 2007; ACCEPTED November 20, 2007)

Abstract

Phenylacetaldehyde dehydrogenase (PAD) and lactaldehyde dehydrogenase (ALD) share some structural and kinetic properties. One difference is that PAD can use NAD^+ and $NADP^+$, whereas ALD only uses NAD^+. An acidic residue has been involved in the exclusion of $NADP^+$ from the active site in pyridine nucleotide-dependent dehydrogenases. However, other factors may participate in $NADP^+$ exclusion. In the present work, analysis of the sequence of the region involved in coenzyme binding showed that residue F180 of ALD might participate in coenzyme specificity. Interestingly, F180T mutation rendered an enzyme (ALD-F180T) with the ability to use $NADP^+$. This enzyme showed an activity of 0.87 μmol/(min * mg) and K_m for $NADP^+$ of 78 μM. Furthermore, ALD-F180T exhibited a 16-fold increase in the V_m/K_m ratio with NAD^+ as the coenzyme, from 12.8 to 211. This increase in catalytic efficiency was due to a diminution in K_m for NAD^+ from 47 to 7 μM and a higher V_m from 0.51 to 1.48 μmol/(min * mg). In addition, an increased K_d for NADH from 175 (wild-type) to 460 μM (mutant) indicates a faster product release and possibly a change in the rate-limiting step. For wild-type ALD it is described that the rate-limiting step is shared between deacylation and coenzyme dissociation. In contrast, in the present report the rate-limiting step in ALD-F180T was determined to be exclusively deacylation. In conclusion, residue F180 participates in the exclusion of $NADP^+$ from the coenzyme binding site and disturbs the binding of NAD^+.

Keywords: ALDHs; aldehyde dehydrogenases; ALD; lactaldehyde dehydrogenase; catalytic efficiency; burst; coenzyme binding domain

Supplemental material: see www.proteinscience.org

Aldehyde dehydrogenases (ALDHs) oxidize aldehydes to their corresponding acids in reactions coupled to the reduction of $NAD(P)^+$. Most ALDHs are NAD^+-dependent enzymes (Perozich et al. 1999; Sophos and Vasiliou 2003), but some use $NADP^+$ (Mann and Weiner 1999; Perozich et al. 2000; Hsu et al. 2001; Cobessi et al. 2000; Ho and Weiner 2005). ALDHs participate in the detoxification of aldehydes, although in a nonspecific manner; therefore, this has been proposed to be their physiological role. However, some ALDHs participate in metabolic pathways or have more specific physiological roles. For instance, ALD and PAD from *Escherichia coli* K12 participate in the degradation pathways of rare carbon sources (Caballero et al. 1983; Hanlon et al. 1997); betaine aldehyde dehydrogenase is involved in osmolarity regulation (Weretilnyk

Reprint requests to: José Salud Rodríguez-Zavala, Departamento de Bioquímica, Instituto Nacional de Cardiología, Tlalpan D.F. 14080, Mexico; e-mail: rodjos@cardiologia.org.mx; fax: 52 55 55 73 09 26.

Abbreviations: ALDHs, aldehyde dehydrogenases; ALD, lactaldehyde dehydrogenase; PAD, phenylacetaldehyde dehydrogenase; Vh-ALDH, Vibrio harveyi aldehyde dehydrogenase; ALDH1, class 1 aldehyde dehydrogenase; ALDH3, class 3 aldehyde dehydrogenase.

Article published online ahead of print. Article and publication date are at http://www.proteinscience.org/cgi/doi/10.1110/ps.073277108.

and Hanson 1990), retinaldehyde dehydrogenase plays a crucial role in cell development and differentiation (Niederreither et al. 2001), and ALDH from *Euglena gracilis* participates in the energy metabolism of this protist (Rodríguez-Zavala et al. 2006b).

The participation of ALDHs in metabolic pathways is widespread in microorganisms. In *E. coli*, more than 17 ALDH genes have been identified (Perozich et al. 1999; Sophos and Vasiliou 2003). Three of these enzymes have been characterized recently: aldB, which has been involved in the removal of toxic alcohols and aldehydes in *E. coli* grown under severe conditions (Ho and Weiner 2005), and ALD and PAD (Rodríguez-Zavala et al. 2006a), which have been identified as part of the degradation pathway of phenylalanine (Hanlon et al. 1997) and of the metabolism of fucose and rhamnose (Caballero et al. 1983; Baldoma and Aguilar 1987; 1988), respectively.

A glutamate at the coenzyme binding domain has been related to the binding and stabilization of NAD^+ in NAD^+-dependent ALDHs (Perozich et al. 2000). It has been shown that this residue interacts with the 2′-hydroxyl of adenosine ribose. However, a Thr or Lys is found at this position in $NADP^+$-dependent ALDHs (Zhang et al. 1999; Ahvazi et al. 2000); these residues stabilize the 2′-phosphate of $NADP^+$. Paradoxically, a negatively charged residue at this position has also been associated with the exclusion of $NADP^+$ from the active site of NAD^+-specific enzymes (Brändén and Tooze 1991). Like most ALDHs, *E. coli* ALD and PAD possess a Glu residue (E179) in the coenzyme binding site domain, which is involved in the stabilization of the adenine ring. The sequences of PAD and ALD around E179 are almost identical, but PAD can use NAD^+ and $NADP^+$ as coenzymes whereas ALD uses only NAD^+ (Rodríguez-Zavala et al. 2006a). Therefore, in the present work, site-directed mutagenesis was carried out to examine the role of the E179 region in the determination of the coenzyme preference in *E. coli* ALD.

Results

Sequence alignment

Sequence alignment of a portion of the coenzyme binding domain around residue E179 (from residue 173 to residue 182) from ALDHs with different coenzyme preference was performed to identify important residue divergences (data not shown). In 10 residues around E179, ALD and PAD sequences are identical except for residue 180, which is Phe in ALD and Thr in PAD (Fig. 1A). As E179 is recognized as an important participant in the binding and stabilization of NAD^+ in most ALDHs (Zhang et al. 1999; Perozich et al. 2000), it was judged relevant to determine the orientation and the interactions of F180 in the active site.

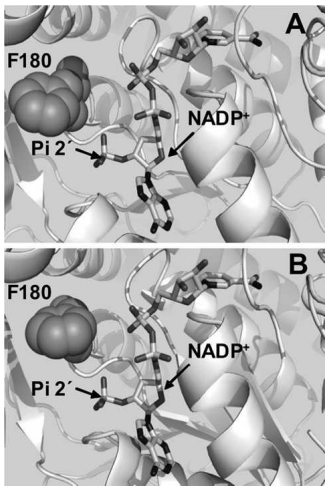

Figure 1. Representation of the interactions of $NADP^+$ and F180 at the coenzyme binding domain of ALD. Panel *A* was built by using a homology model obtained for ALD and Panel *B* was obtained by aligning the three-dimensional model generated for ALD with the published structure of ALD to introduce $NADP^+$ into the coenzyme binding site (Di Costanzo et al. 2007). This figure was generated with PyMOL (http://pymol.sourceforge.net/) and Spdbv (http://www.expasy.org/spdbv/).

Modeling of the tertiary structures of ALD

An ALD three-dimensional model was built by using as template the structure of the *E. coli* NAD^+-dependent medium-chain aldehyde dehydrogenase (1WNB), which showed the highest sequence identity with ALD (38.5%). According to its sequence identity, 1WNB is a member of the betaine aldehyde dehydrogenase family (Gruez et al. 2004). The ALD model was initially generated with NAD^+ at the active site (data not shown), as this is the coenzyme found in the 1WNB structure.

Since the interest of this work was to evaluate the inability of ALD to use $NADP^+$, it was imperative to generate a model of the enzyme with this coenzyme at the active site. For that purpose, different structures containing $NADP^+$ were used as templates to model ALD. The template proteins were (1) the three-dimensional structure of ALD generated with 1WNB as the template; (2) two structures of the *Streptococcus mutants* $NADP^+$-dependent aldehyde dehydrogenase 2euhA (Cobessi et al. 1999) and 1qi1A (Cobessi et al. 2000), which showed 32.3% and 32.6% sequence identity with ALD, respectively; and (3) the structure of the nonphosphorylating glyceraldehyde-3-phosphate dehydrogenase 1ky8A (Pohl et al. 2002), which has 31.7% sequence identity with ALD. The ALD model generated with $NADP^+$ at the active site (Fig. 1A) revealed that residue F180 was at

a distance of 3.4 Å from the 2′-phosphate of $NADP^+$, which suffices to perturb its binding. This observation led me to hypothesize that residue F180 may exert a steric effect, which impairs $NADP^+$ binding to the active site, and, thus, this residue affects coenzyme specificity.

The structure of *E. coli* ALD was recently solved, and two crystals of the enzyme were obtained, one with NADH and another with NADPH in the active site (Di Costanzo et al. 2007). To further explore the F180 interactions, the model here generated was aligned with the ALD crystal structure to introduce $NADP^+$ into the active site (Fig. 1B). This alignment showed that, in the crystal, F180 was at 4 Å from the 2′ phosphate of $NADP^+$ and, thus, it could indeed be exerting a steric effect on this coenzyme at the active site.

Kinetic characterization of ALD-F180T

To promote the binding of $NADP^+$ to ALD, residue F180 was mutated to T, as this was the residue found at the same position in PAD, which is able to use both coenzymes (Rodríguez-Zavala et al. 2006a). The mutant protein (ALD-F180T) was purified to homogeneity and the kinetic parameters were determined. Indeed, ALD-F180T showed significant activity with $NADP^+$, which was higher than that attained with NAD^+ (Table 1); the K_{ia} (constant related to the K_d for $NADP^+$) value of ALD-F180T for $NADP^+$ revealed high affinity, whereas the K_m value for $NADP^+$ was 11 times higher than that for NAD^+ (Fig. 2A). Thus, the catalytic efficiency (V_m/K_m) of the mutant enzyme with $NADP^+$ was similar to that reached by the wild-type enzyme with NAD^+. Surprisingly, V_m of ALD-F180T with NAD^+ was threefold higher and K_m for NAD^+ was sixfold lower than those of ALD wild type (Table 1). Hence, the catalytic efficiency of the mutant with NAD^+ was 17-fold higher than that of ALD wild type. The K_{ia} value for NAD^+ of ALD-F180T (Fig. 2B; Table 1) was 12-fold lower than that reported for wild-type ALD (79 μM) (Rodríguez-Zavala et al. 2006a), indicating an increase in NAD^+ affinity in the mutant.

Thermal stability studies

Experiments of protection against thermal denaturalization were performed to test whether the lack of activity of wild-type ALD with $NADP^+$ was related to its inability to bind this coenzyme. $NADP^+$ (1 mM) did not protect wild-type ALD against thermal denaturalization (Fig. 2C), suggesting no $NADP^+$ binding, whereas incubation of ALD with 1 mM NAD^+ did protect the enzyme. In contrast, $NADP^+$ protected ALD-F180T (Fig. 2C), and this protection was similar to that induced by NAD^+ on the ALD wild type (Fig. 2D). Interestingly, the protection against thermal denaturalization by NAD^+ was higher in ALD-F180T than in wild-type ALD (Fig. 2D).

Presence of pre-steady-state burst

The increase in V_m shown by the mutant enzyme could be related to a change in the rate-limiting step. Pre-steady-state burst analysis was performed with the mutant to determine whether the rate-limiting step was still located after the NADH formation step, as reported for ALD wild type (Rodríguez-Zavala et al. 2006a). ALD-F180T exhibited a pre-steady-state burst (data not shown) indicating that the rate-limiting step remained after the NADH formation (see reaction sequence in Fig. 3). The magnitude of the burst was 2 nmol NADH/nmol enzyme, as determined for ALD wild type (Rodríguez-Zavala et al. 2006a) and for other tetrameric enzymes (Wang and Weiner 1995; Weiner et al. 1976).

Determination of the rate-limiting step

The presence of a pre-steady-state burst discarded the hydride transfer (k5 in Fig. 3) as the rate-limiting step and indicated that this should be located after the formation of NADH, either at the deacylation or the coenzyme dissociation. For ALD wild type, it was previously shown that both deacylation and coenzyme dissociation contribute to limit the reaction rate (Rodríguez-Zavala et al. 2006a). Studies with human enzymes have shown that

Table 1. *Kinetic parameters of the mutant ALD-F180T*

	ALD WT			ALD-F180T		
	Propional	NAD^+	$NADP^+$	Propional	NAD^+	$NADP^+$
K_m (mM)	0.25 ± 0.06	0.04 ± 0.02	NA	0.26 ± 0.04	0.007 ± 0.004	0.078 ± 0.03[a]
V_m μmol/(min * mg)	0.52 ± 0.08	0.51 ± 0.13	ND	1.47 ± 0.16	1.48 ± 0.18	0.87 ± 0.15[a]
V_m/K_m	2.1	12.8	NA	5.7	211	11.2
K_{ia} (mM)	NA	0.079 ± 0.006[b]	NA	NA	0.0065 ± 0.005	0.33 ± 0.045

Results are the mean ± *SD* of four different determinations except as noted.
[a] Five determinations were used.
[b] Value was taken from Rodríguez-Zavala et al. (2006a).
(ND) not detected; (NA) not applicable.

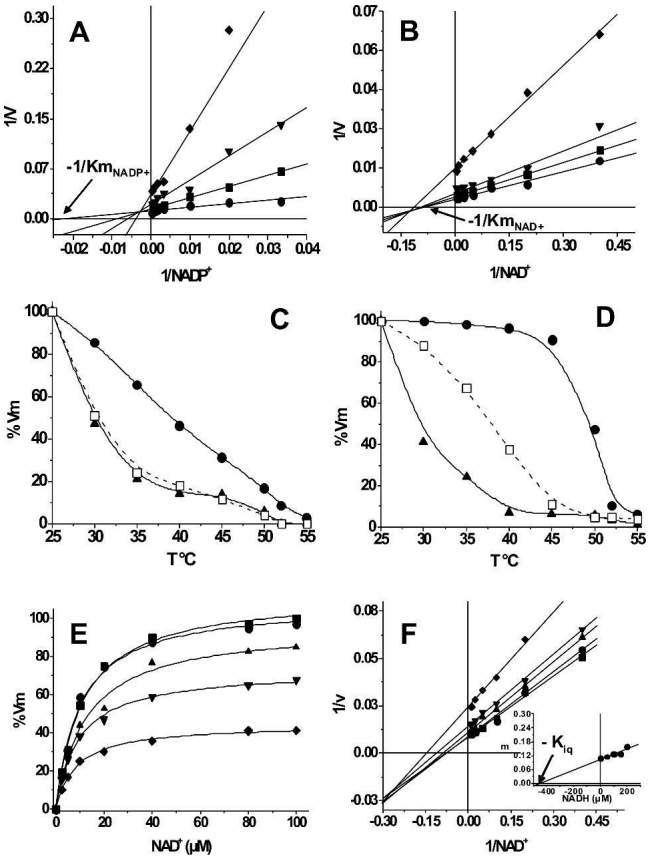

Figure 2. Kinetic characterization and thermal stability assays of ALD-F180T. The kinetic parameters were obtained as described in Materials and Methods. Plots shown are representative of five different determinations for $NADP^+$ and four determinations for NAD^+ and NADH. (*A*) Kinetic parameters for $NADP^+$ were obtained by varying propionaldehyde concentration as follows: ●, 2; ■, 0.25; ▼, 0.1; and ◆, 0.05 μM. (*B*) Kinetic parameters for NAD^+ were determined varying propionaldehyde as follows: ●, 2; ■, 0.5; ▼, 0.25; and ◆, 0.05 μM. K_m and K_{ia} values obtained from these data are shown in Table 1. (*C*,*D*) Protection of ALD and ALD-F180T against thermal denaturalization by the coenzyme. (▲) Enzyme incubated without coenzyme; (□) enzyme incubated with 1 mM $NADP^+$; (●) enzyme incubated with 1 mM NAD^+. Activity of ALD incubated with $NADP^+$ was then assayed with 1 mM NAD^+. These plots are representative of results obtained with three different enzyme preparations. (*E*,*F*) Determination of the K_{iq} of ALD-F180T. NAD^+ kinetics were carried out in the presence of 1 mM propionaldehyde and in the absence (■) or in the presence of the following NADH concentrations: ●, 50; ▲, 100; ▼, 150; and ◆, 200 μM. Plots are representative of four different determinations and two enzyme preparations. The *inset* in *F* is the secondary plot of the slopes of the lines against the NADH concentrations. K_{iq} value represents the mean ± *SD* of four different determinations. K_{iq} = 466 ± 60 μM.

magnesium affects differentially the kinetic steps of ALDH located after NADH formation. This ion increases the hydrolysis rate of the acyl intermediate (k7 in Fig. 3; Wang and Weiner 1995) and decreases the rate of coenzyme dissociation (k9 in Fig. 3; Takahashi and Weiner 1980; Ho et al. 2005). When the ALD-F180T activity was assayed in the presence of 2 mM Mg^{2+} (Table 2), no effect on V_m was attained. This Mg^{2+} concentration inhibits the activity of ALD wild type by 50% (Rodríguez-Zavala et al. 2006a).

The K_{iq} constant, a value equivalent to K_d for NADH, was determined to define the modification of the rate-limiting step in the mutant enzyme. The K_{iq} value determined was 466 ± 60 μM (n = 3) (Fig. 2E,F), a value 3.1-fold higher than the K_{iq} obtained for ALD wild type (150 ± 27 μM) (Rodríguez-Zavala et al. 2006a). This higher value for K_{iq} could account for the threefold increase in V_m in the mutant. Furthermore, activity assays with aldehydes with electron-withdrawing and electron-donating substituent groups were made in order to provide an alternative way to assess the rate-limiting step of ALD-F180T. p-Nitrobenzaldehyde was oxidized more rapidly than benzaldehyde or p-methoxybenzaldehyde by ALD-F180T (Table 3), indicating that deacylation was rate limiting.

Discussion

Data from the structure of the binary complex of ALD with NADPH indicate that the negatively charged carboxylate group of E179 destabilizes the binding of the 2′-phosphate of NADPH, thus hampering enzyme activity with this coenzyme (Di Costanzo et al. 2007). However, data of the present work (cf. Table 1, Fig. 2) indicate that other factors are involved in the exclusion of $NADP^+$ from the active site. In particular, mutating F180 by T permitted $NADP^+$ binding and utilization, as revealed by the activity exhibited by ALD-F180T with this coenzyme (Table 1) and the improved binding of NAD^+ to the enzyme, as indicated by the 6-fold increment in the affinity and the 12-fold diminution in the K_d for this coenzyme as compared to ALD wild-type (Table 1; Fig. 2A,B). Moreover, $NADP^+$ protected the mutant

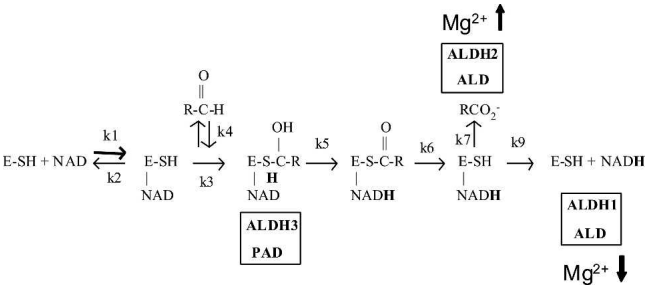

Figure 3. Diagram of the general mechanism of reaction of ALDHs.The rate-limiting step is indicated for some ALDHS: Hydride transfer (k5) is the rate-determining step for ALDH3 and PAD; deacylation (k7) is the rate-limiting step for ALDH3 and partially for ALD; coenzyme dissociation is the rate-determining step for ALDH1 and partially for ALD. Activation by Mg^{2+} on the deacylation step is indicated by an upward arrow, while Mg^{2+} inhibiting effect on coenzyme dissociation is indicated by a downward arrow.

Table 2. *Effect of Mg^{2+} ions on the activity of ALD-F180T*

	V_m μmol/(min * mg)	
	$-Mg^{2+}$	+2 mM Mg^{2+}
ALD	0.57 ± 0.04	0.28 ± 0.07
ALD-F180T	1.50 ± 0.08	1.57 ± 0.06

Results are the mean ± *SD* of four different experiments.

enzyme against thermal denaturalization (Fig. 2D), which was not achieved with wild-type ALD (Fig. 2C). NAD^+ protection was higher in ALD-F180T than in wild-type ALD, suggesting that the binding of NAD^+ to the mutant enzyme was more efficient than its binding to ALD, which agrees with the lower K_m and K_d values of ALD-F180T for NAD^+ (Table 1; Fig. 2B). It was surprising that the mutation did not decrease enzyme stability (Fig. 2D). Some reports indicate that single mutations at the coenzyme binding site (Ho and Weiner 2005; Ho et al. 2006) or in regions other than the active site can modify this domain and are accompanied by a detriment in enzyme stability and activity (Rodríguez-Zavala and Weiner 2001, 2002).

The involvement of other factors in the determination of the coenzyme specificity has been demonstrated for other ALDHs. Mutation of T175 of Vh-ALDH to a negatively charged amino acid displaced the preference from $NADP^+$ to NAD^+ and increased the catalytic efficiency, while changing this residue to Gln, created a more efficient NAD^+-enzyme without loss of $NADP^+$-dependent activity (Zhang et al. 1999). On the other hand, an acidic residue at this position has been associated with the exclusion of $NADP^+$ from the active site of NAD^+-specific enzymes (Brändén and Tooze 1991). This glutamate residue is found at position 179 in over two thirds of ALDH sequences, and only some are able to use $NADP^+$ as coenzyme. The ALDH3 family, despite possessing Glu at the active site, can use either NAD^+ or $NADP^+$. Mutation of residue E140 of rat ALDH3 (for this enzyme, residue numbering changes, as it does not have 56 amino acids at the N terminus as compared to tetrameric ALDHs; Liu et al. 1997; Perozich et al. 1999; Rodríguez-Zavala and Weiner 2001) to Asn, Asp, Thr, or Gln enhances the preference for $NADP^+$ (Perozich et al. 2000). In addition to E140, which contributes to the tight binding of NAD^+, it has been proposed that K137 (highly conserved residue in more than 97% of the ALDH sequences) is essential for binding both coenzymes (Perozich et al. 2000). Nevertheless, in these works, complete abolishment of the use of either coenzyme was unsuccessful, indicating that additional factors contribute to the ability of these enzymes to utilize $NADP^+$.

The repulsion effect between the negatively charged groups of $NADP^+$ and E179 is evident from ALD structure data (Di Costanzo et al. 2007). Substituting Phe180 for Thr seems to generate a cavity in the active site, which might allow the side chain of Glu179 to move away from 2′-phosphate of $NADP^+$, thus permitting the adequate coupling of this coenzyme to the active site (Fig. 4B).

The increase in activity of ALD-F180T with NAD^+ with respect to wild-type ALD might be induced by the change in the rate-limiting step, which is shared between deacylation and coenzyme dissociation in ALD wild type. A change in the rate-limiting step was indeed demonstrated by the absence of Mg^{2+} inhibitory effect on ALD-F180T activity (Table 2). This finding indicates that, for ALD-F180T, NADH dissociation was no longer rate limiting. This observation was further supported by the higher activity obtained with p-nitrobenzaldehyde as compared with that obtained with benzaldehyde (Figs. 3,4; Table 3). The fact that the nitro derivative was oxidized more rapidly is consistent with a nucleophilic attack contributing to the rate-limiting step. Thus, unlike ALD wild type, in ALD-F180T, deacylation is the only rate-limiting step.

Changes in the rate-limiting step by site-directed mutagenesis at the active site of ALDH have been described (Ho et al. 2005, 2006). Mutation of E399 in human ALDH1 changes the rate-limiting step from coenzyme dissociation in ALDH1 wild type (MacGibbon et al. 1977) to hydride transfer in the mutant (Ho et al. 2005), as well as in ALDH3 (Mann and Weiner 1999) and *E. coli*. PAD (Rodríguez-Zavala et al. 2006a). Furthermore, mutation of T244 to Ser in human ALDH1 rendered an enzyme in which the rate-limiting step changed from coenzyme dissociation to deacylation. The change in rate-limiting step allows changing the inhibitory effect of Mg^{2+} on ALDH1 wild type to an activating effect on the ALDH1-T244S mutant (Ho et al. 2006).

The increase in NADH K_{iq} (i.e., $K_d = k_{off}/k_{on}$) from 150 in the native ALD (Rodríguez-Zavala et al. 2006a) to 466 μM in ALD-F180T (Fig. 3D,E) indicates a faster coenzyme release, and, hence, this step may no longer be rate limiting. Moreover, this increase of about threefold in the K_d of ALD-F180T for NADH could account for the threefold increment in the mutant enzyme V_m.

Table 3. *Activity of ALD-F180T with benzaldehyde and some derivatives*

	V_m μmol/(min * mg)		
	Benzaldehyde	p-Nitro-benzaldehyde	p-Methoxy-benzaldehyde
ALD	0.25 ± 0.04	2.1 ± 0.14	0.11 ± 0.04
ALD-F180T	0.31 ± 0.02	3.2 ± 0.19	0.46 ± 0.03

Results are the mean ± *SD* of four different experiments and two enzyme preparations.

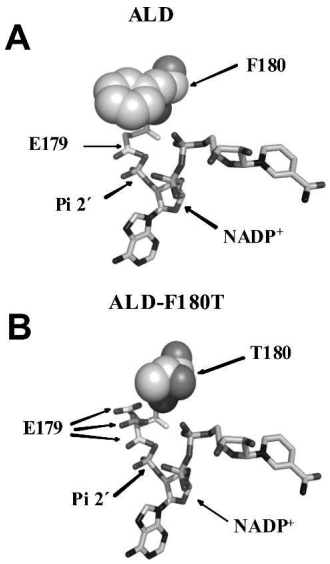

Figure 4. Comparison of the coenzyme binding site of ALD and ALD-F180T. (*A*,*B*) F180 and T180 are shown as spheres, while E179 and $NADP^+$ are shown as sticks. E179 is shown in three different positions moving away from E179 and toward T180. Figures were generated using the reported ALD structure (Di Costanzo et al. 2007), with PyMOL (http://pymol.sourceforge.net/) and Spdbv (http://www.expasy.org/spdbv/).

In general, the NAD^+ pool is used by enzymes involved in catabolic pathways, whereas the $NADP^+$ pool is used for biosynthesis. The presence of the Phe residue at the active site of ALD might be a strategy to restrict the use of the $NADP^+$ pool by this enzyme in *E. coli*. By performing a BLAST analysis with the sequence of *E. coli* lactaldehyde dehydrogenase, another four ALDHs possessing Phe at position 180 can be found. These enzymes are all found in bacteria that belong to the enterobacteriales (Fig. 5). The sequence identity observed among these enzymes was 83%–85% (data not shown), which indicates that they might share a common ancestor. Therefore, considering the data of the present work (E180 is key for the exclusion of $NADP^+$ from the active site of *E. coli* ALD, and this residue determines the coenzyme preference in this enzyme), it is predicted that these enzymes are unable to bind and use $NADP^+$ as coenzyme.

Materials and Methods

Expression and purification of the recombinant enzymes

The plasmids containing the DNA encoding the ALD protein were kindly provided by Dr. Henry Weiner from the Department of Biochemistry, Purdue University. This sequence was subcloned into a vector to add a His-Tag to the N terminus of the protein to facilitate the purification (Mann and Weiner 1999). Introduction of the mutations was performed by PCR using synthetic oligonucleotides, as described (Ho et al. 1989). *E. coli* BL21 (DE3)pLysS strain was transformed with the vectors containing the His-Tag constructs. The proteins were overexpressed as reported elsewhere (Rodríguez-Zavala and Weiner 2002). The cells were harvested and washed twice with 100 mL saline solution. Then, the cells were disrupted by sonication at 4°C and the extract was centrifuged at 100,000*g* for 1 h. The supernatant containing the recombinant protein was applied to a 20-mL Chelating-Sepharose column packed with $NiCl_2$ and equilibrated with a buffer containing 50 mM H_2NaPO_4 (pH 7.5), 500 mM NaCl, and 20 mM 2-mercaptoethanol at 4°C. The column was washed with 50 mM imidazole in the same buffer, and the protein was eluted applying a 100-mL total volume of a 50–500 mM linear imidazole gradient. Fractions with activity were pooled, concentrated using Amicon filters of 50,000 kDa MWCO, and washed with a buffer containing 100 mM H_2NaPO_4 (pH 7.5), 100 mM NaCl, and 0.025% 2-mercaptoethanol to eliminate imidazol. The pure enzyme was then concentrated and stored at −20°C in the presence of 50% glycerol until use. Protein stored this way was stable for more than 6 mo. The protein concentration was determined with the bicinchoninic acid protein assay kit (Sigma-Aldrich), using bovine serum albumin as standard. The enzyme purified this way had a purity of more than 95% as judged from SDS-PAGE gels (Laemmli 1970).

Activity assay

For the determination of the activity, 20 μg of protein were added to a buffer containing 100 mM H_2NaPO_4 (pH 7.5), 100 mM NaCl, 20 mM 2-mercaptoethanol, and 1 mM NAD^+ or 1 mM $NADP^+$. The reaction was initiated by the addition of aldehyde. The ALDH activity was measured with the use of a Turner SP-830 spectrophotometer, following the increase in absorbance at 340 nm due to the formation of NADH. The dissociation constants of NADH (K_{iq}) were determined as inhibition constants using NADH as a competitive inhibitor against NAD^+, with propionaldehyde as the substrate. K_{ms}, K_{ia}, and K_{iq} values were determined from the secondary plots (slope vs. the inverse of coenzyme concentration) of the Lineweaver Burk graphs of the double substrate kinetics shown in Figure 2. In these secondary plots, K_{ia} and K_{iq} are calculated from the abscissa to the origin. The rate equation for a Bi–Bi ordered reaction is

$$\frac{1}{v} = \frac{K_{mB}}{V_{\max}}\left(1 + \frac{K_{ia}}{[A]}\right)\frac{1}{B} + \frac{1}{V_{\max}}\left(1 + \frac{K_{mA}}{[A]}\right)$$

where A is NAD^+, B is propionaldehyde, K_{mA} is K_m for NAD^+, K_{mB} is K_m for propional, and K_{ia} is K_d for NAD^+.

```
                        R171                F180                G200
Escherichia coli        RKMAPALLTG NTIVIKPSEF TPNNAIAFAK IVDEIGLPRG
Shigella flexneri       RKMAPALLTG NTIVIKPSEF TPNNAIAFAK IVDEIGLPRG
Enterobacter sp.        RKLAPALLTG NTIVIKPSEF TPNNAIAFAK IVDDIGLPKG
Citrobacter koseri      RKLAPALLTG NTIVIKPSEF TPNNAIAFAQ IVHDIGLPKG
Klebsiella pneumoniae   RKLAPALITG NTIVIKPSEF TPNNAIAFAQ IVHDIGLPKG
```

Figure 5. Alignment of the amino acid sequence of the F180 region of ALDHs of some enterobacteriales. The alignment of these sequences showed 83%–85% identity with ALD. Residues E179 and F180 are shown in a rectangle. F180 is in bold lettering.

Thermal denaturalization assays

Protein (200 μg) was incubated at the indicated temperature in the absence or in the presence of the coenzyme for 5 min. Then, an aliquot (20 μg) was poured into a cuvette containing the assay buffer at 25°C for activity measurement.

Determination of the pre-steady-state burst

The pre-steady-state burst magnitude of NADH formation was determined by the use of an Aminco Bowman Series 2 spectrofluorometer (SLM-AMINCO Instruments, Inc.) as reported previously (Farrés et al. 1994). The protein (10–20 μM) was incubated in a buffer composed of 100 mM H_2NaPO_4 (pH 7.4), 100 mM NaCl, and 2 mM NAD^+. The reaction was started by the addition of propionaldehyde. The magnitude of the burst of NADH formation was calculated extrapolating the linear portion of the steady-state rate of the reaction to the time of the addition of the substrate. This value was correlated with a calibration curve generated with NADH.

Modeling of the tertiary structures and sequence alignment

Models of the ALD were obtained using the SWISS-MODEL software (available at http://swissmodel.expasy.org/) (Peitsch 1995; Guex and Peitsch 1997; Schwede et al. 2003). Analysis of the structures and generation of the figures were performed with the Protein Explorer program (free software by Erick Martz), the Spdbv software (http://www.expasy.org/spdbv/; Guex and Peitsch 1997), and PyMOL (http://pymol.sourceforge.net/). Sequence alignments were made using the MultiAlign interface by Florence Corpet (Corpet 1988) and the Tcoffe Server (Notredame et al. 2000; Poirot et al. 2003).

Electronic supplemental material

Supplemental Figure 1A shows the alignment of the sequence of the coenzyme binding site of ALDHs with different coenzyme preference and highlights residue F180 in ALD. Supplemental Figure 1B shows the location of F180 with respect to $NADP^+$ in the active site of the ALD model; Supplemental Figure 2 shows the presence of pre-steady-state burst in ALD-F180T mutant. Supplemental Figure 3 shows the cavity formed in the active site of ALD when residue F180 is mutated to T, which facilitates the movement of NADH or NADPH out of the coenzyme binding site.

References

Ahvazi, B., Coulombe, R., Delarge, M., Vedadi, M., Zhang, L., Meighen, E., and Vrielink, A. 2000. Crystal structure of the NADP+-dependent aldehyde dehydrogenase from *Vibrio harveyi*: Structural implications for cofactor specificity and affinity. *Biochem. J.* **349:** 853–861.

Baldoma, L. and Aguilar, J. 1987. Involvement of lactaldehyde dehydrogenase in several metabolic pathways of *Escherichia coli* K12. *J. Biol. Chem.* **262:** 13991–13996.

Baldoma, L. and Aguilar, J. 1988. Metabolism of L-fucose and L-rhamnose in *Escherichia coli*: Aerobic–anaerobic regulation of L-lactaldehyde dissimilation. *J. Bacteriol.* **170:** 416–421.

Brändén, C. and Tooze, J. 1991. Introduction to protein structure. Garland, New York.

Cabellero, A., Baldoma, L., Ros, J., Boronat, A., and Aguilar, J. 1983. Identification of lactaldehyde dehydrogenase and glycolaldehyde dehydrodenase as functions of the same protein in *Escherichia coli*. *J. Biol. Chem.* **258:** 7788–7792.

Cobessi, D., Tete-Favier, F., Marchal, S., Azza, S., Branlant, G., and Aubry, A. 1999. Apo and holo crystal structures of an NADP-dependent aldehyde dehydrogenase from *Streptococcus* mutants. *J. Mol. Biol.* **290:** 161–173.

Cobessi, D., Tête-Favier, F., Marchal, S., Branlant, G., and Aubry, A. 2000. Structural and biochemical investigations of the catalytic mechanism of an NADP-dependent aldehyde dehydrogenase from *Streptococcus mutans*. *J. Mol. Biol.* **300:** 141–152.

Corpet, F. 1988. Multiple sequence alignment with hierarchical clustering. *Nucleic Acids Res.* **16:** 10881–10890.

Di Costanzo, L., Gomez, G.A., and Christianson, D.W. 2007. Crystal structure of lactaldehyde dehydrogenase from *Escherichia coli* and interferences regarding substrate and cofactor specificity. *J. Mol. Biol.* **366:** 481–493.

Farrés, J., Wang, X., Takahashi, K., Cunningham, S.J., Wang, T.T., and Weiner, H. 1994. Effects of changing glutamate 487 to lysine in rat and human liver mitochondrial aldehyde dehydrogenase. *J. Biol. Chem.* **269:** 13854–13860.

Gruez, A., Roig-Zamboni, V., Grisel, S., Salomoni, A., Valencia, C., Campanacci, V., Tegoni, M., and Cambillau, C. 2004. Crystal structure and kinetics identify *Escherichia coli* YdcW gene product as a medium-chain aldehyde dehydrogenase. *J. Mol. Biol.* **343:** 29–41.

Guex, N. and Peitsch, M.C. 1997. SWISS-MODEL and the Swiss-PdbViewer: An environment for comparative protein modelling. *Electrophoresis* **18:** 2714–2723.

Hanlon, S.P., Hill, T.K., Flavell, M.A., Stringfellow, J.M., and Cooper, R.A. 1997. 2-Phenylethylamina catabolism by *Escherichia coli* K-12: Gene organization and expression. *Microbiol.* **143:** 513–518.

Ho, K.K. and Weiner, H. 2005. Isolation and characterization of an aldehyde dehydrogenase encoded by the aldB gene of *Escherichia coli*. *J. Bacteriol.* **187:** 1067–1073.

Ho, S.N., Hunt, H.D., Horton, R.M., Pullen, J.K., and Pease, L.R. 1989. Site-directed mutagenesis by overlap extension using the polymerase chain reaction. *Gene* **77:** 51–59.

Ho, K.K., Allali-Hassani, A., Hurley, T.D., and Weiner, H. 2005. Differential effects of Mg2+ ions on the individual kinetic steps of human cytosolic and mitochondrial aldehyde dehydrogenases. *Biochemistry* **44:** 8022–8029.

Ho, K.K., Hurley, T.D., and Weiner, H. 2006. Selective alteration of the rate-limiting step in cytosolic aldehyde dehydrogenase through random mutagenesis. *Biochemistry* **45:** 9445–9453.

Hsu, L.C., Shibuya, A., and Yoshida, A. 1992. Human stomach aldehyde dehydrogenase cDNA and genomic cloning, primary structure, and expression in *Escherichia coli*. *J. Biol. Chem.* **267:** 3030–3037.

Laemmli, U.K. 1970. Cleavage of structural proteins during the assembly of the head of bacteriophage T4. *Nature* **227:** 680–685.

Liu, Z.J., Sun, Y.J., Rose, J., Chung, Y.J., Hsiao, C.D., Chang, W.R., Kuo, I., Perozich, J., Lindahl, R., Hempel, J., et al. 1997. The first structure of an aldehyde dehydrogenase reveals novel interactions between NAD and the Rossmann fold. *Nat. Struct. Biol.* **4:** 317–326.

MacGibbon, A.K., Buckey, P.D., and Blackwell, L.F. 1977. Evidence for two step binding of reduced nicotinamide-adenine dinucleotide to aldehyde dehydrogenase. *Biochem. J.* **165:** 455–462.

Mann, C.J. and Weiner, H. 1999. Differences in the roles of conserved glutamic acid residues in the active site of human class 3 and class 2 aldehyde dehydrogenases. *Protein Sci.* **8:** 1922–1929.

Niederreither, K., Vermot, J., Messaddeq, N., Schuhbaur, B., Chambon, P., and Dollé, P. 2001. Embryonic retinoic acid synthesis is essential for heart morphogenesis in the mouse. *Development* **128:** 1019–1031.

Notredame, C., Higgins, D.G., and Heringa, J. 2000. T-Coffee: A novel method for fast and accurate multiple sequence alignment. *J. Mol. Biol.* **302:** 205–217.

Peitsch, M.C. 1995. Protein modeling by E-mail. *Biotechnology* **13:** 658–660.

Perozich, J., Nicholas, H., Lindahl, R., and Hempel, J. 1999. The big book of aldehyde dehydrogenase sequences. An overview of the extended family. *Adv. Exp. Med. Biol.* **463:** 5–52.

Perozich, J., Kuo, I., Wang, B.C., Boesch, J.S., Lindahl, R., and Hempel, J. 2000. Shifting the NAD/NADP preference in class 3 aldehyde dehydrogenase. *Eur. J. Biochem.* **267:** 6197–6203.

Pohl, E., Brunner, N., Wilmanns, M., and Hensel, R. 2002. The crystal structure of the allosteric non-phosphorylating glyceraldehyde-3-phosphate dehydrogenase from the hyperthermophilic archaeum *Thermoproteus tenax*. *J. Biol. Chem.* **277:** 19938–19945.

Poirot, O., O'Toole, E., and Notredame, C. 2003. Tcoffee@igs: A web server for computing, evaluating and combining multiple sequence alignments. *Nucleic Acids Res.* **31:** 3503–3506.

Rodríguez-Zavala, J.S. and Weiner, H. 2001. Role of the C-terminal tail on the quaternary structure of aldehyde dehydrogenases. *Chem. Biol. Interact.* **130:** 151–160.

Rodríguez-Zavala, J.S. and Weiner, H. 2002. Structural aspects of aldehyde dehydrogenase that influence dimer-tetramer formation. *Biochemistry* **41:** 8229–8237.

Rodríguez-Zavala, J.S., Allali-Hassani, A., and Weiner, H. 2006a. Characterization of *E. coli* tetrameric aldehyde dehydrogenases with atypical properties compared to other aldehyde dehydrogenases. *Protein Sci.* **15:** 1387–1396.

Rodríguez-Zavala, J.S., Ortíz-Cruz, M.A., and Moreno-Sánchez, R. 2006b. Characterization of an aldehyde dehydrogenase from *Euglena gracilis*. *J. Eukaryot. Microbiol.* **53:** 36–42.

Schwede, T., Kopp, J., Guex, N., and Peitsch, M.C. 2003. SWISS-MODEL: An automated protein homology-modeling server. *Nucleic Acids Res.* **31:** 3381–3385.

Sophos, N.A. and Vasiliou, V. 2003. Aldehyde dehydrogenase gene superfamily: The 2002 update. *Chem. Biol. Interact.* **143–144:** 5–22.

Takahashi, K. and Weiner, H. 1980. Magnesium stimulation of catalytic activity of horse liver aldehyde dehydrogenase. Changes in molecular weight and catalytic sites. *J. Biol. Chem.* **255:** 8206–8209.

Wang, X.P. and Weiner, H. 1995. Involvement of glutamate 268 in the active site of human liver mitochondrial (class 2) aldehyde dehydrogenase as probed by site-directed mutagenesis. *Biochemistry* **34:** 237–243.

Weiner, H., Hu, J.H., and Sanny, C.G. 1976. Rate-limiting steps for the esterase and dehydrogenase reaction catalyzed by horse liver aldehyde dehydrogenase. *J. Biol. Chem.* **251:** 3853–3855.

Weretilnyk, E.A. and Hanson, A.D. 1990. Molecular cloning of a plant betainealdehyde dehydrogenase, an enzyme implicated in adaptation to salinity and drought. *Proc. Natl. Acad. Sci.* **87:** 2745–2749.

Zhang, L., Ahvazi, B., Szittner, R., Vrielink, A., and Meighen, E. 1999. Change of nucleotide specificity and enhancement of catalytic efficiency in single point mutant of *Vibrio harveyi* aldehyde dehydrogenase. *Biochemistry* **38:** 11440–11447.